International Journal of Application or Innovation in Engineering & Management (IJAIEM)
Web Site: www.ijaiem.org Email: editor@ijaiem.org
Volume 6, Issue 6, June 2017 **ISSN 2319 - 4847**

An experimental analysis on the coupling effect of centerwall location and side walls orientation on impinging flow jets

[1]Ezhil Manickam, [2]Pratik Tiwari, [3]Shitiz Sehgal, [4]Ajay Babusekar , [5*]Vinayak Malhotra

[1,2,3,4]B. Tech Student, Dept. of Aerospace Engineering, SRM University, Chennai, Tamil Nadu, India

[5*]Assistant Professor, Dept. of Aerospace Engineering, SRM University, Chennai, Tamil Nadu, India

ABSTRACT

The work aims at understanding the effect of coupling of central wall location and side walls orientation on flow characteristics of an impinging flow jet. The study experimentally intends physical insight into heterogeneous phenomena of efflux from a small opening impinging on a surface confined from three sides under deviant conditions. Systematic experiments were performed on a cascade tunnel with flow ejected at a velocity of 36 m/s. Results show that outside the core region, the flow experiences a monotonic reduction with increase in distance along streamline and radial direction. The flow features vary distinctly with three wall configurations than conventional wall jet. The centerwall location is more efficient in bringing substantial change when placed closer to the exit (low velocity losses) and primarily governs the chances of strong flow deflection or back flow losses. However, wall placed far away from exit results in diminishing returns with a critical value beyond which the flow characteristics become insensitive. The presence of walls on sides results in reduction in the core region. The geometry was noted to influence the entrainment of ambient fluid, the spread of the shear layer and the length of the potential core.

Keywords: Impinging flowjet, wall orientation, wall location, shear interaction, vortices.

1. INTRODUCTION

Flow jets are flow issued from a small opening at a high velocity and represents an imperative area of research interest. The phenomenon covers wide range of practical and engineering applications including space propulsion, boundary-layer separation control, heat transfer as a method of achieving particularly high heat transfer coe□cients, in drying processes, air curtains for room conditioning, heating and ventilating applications. Flow jets are broadly studied under three categories, viz., free jet, wall jet, and impinging jet. This classification is based on presence of a solid surface (i.e. wall) against the jet expelled. In free jet configuration, the jet is issued into an unbounded fluid (stationary or moving). The impinging jet refers to jet striking a plane solid surface in its path at any given orientation. The phenomenon finds application in problems as the mixing and combustion of atomized liquid fuel, jet cooling of commercial products, and the problems associated with jets issuing from rockets or vertical take-off and landing aircraft. The wall jet, which issues tangentially to a plane surface is regarded as a limiting case of impinging jets with zero angle of impingement and finds applications in heat transfer, thrust reversal, mostly fluid structure interactions. Free jets can be defined as a pressure driven unrestricted flow of a fluid into a quiescent ambience. Figure 1(a) shows a free jet issued from a small opening. As the fluid moves downstream, it interacts with the surrounding fluid and momentum drops. Subsequently, the jet efflux splits into three regions viz., core, entrainment, termination, all related to centerline velocity decay (figure 1(b)).

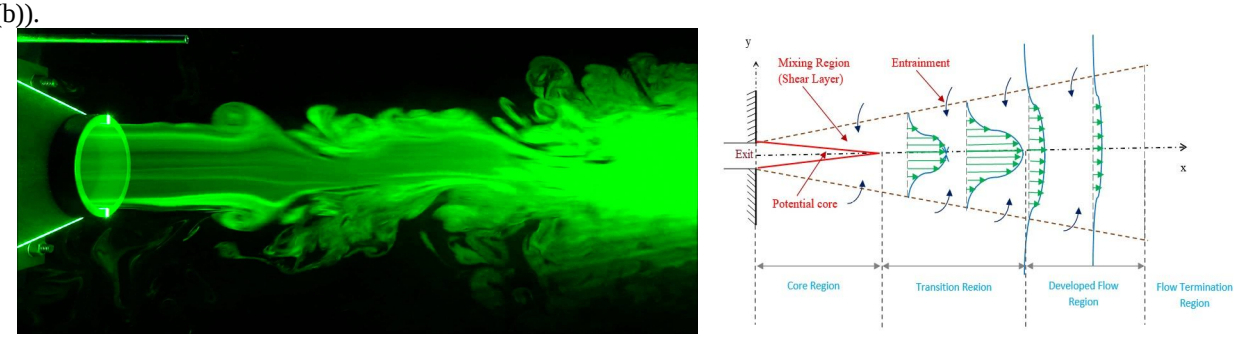

(a) (b)

Figure 1: (a) Pictorial view of a flow jet (b) Schematic of flow structure of a free jet.

In potential core region, the centerline velocity is almost equal to the exit or outlet velocity. This region normally extends up to 4d to 6d, where d is the diameter of the nozzle exit. In entrainment region, fluid comprehensively interacts with the surrounding fluid and is identified by drastic change in flow characteristics. Shear layer is the region in which most of the interactions and mixing between the ambient and jet fluids take place. The entrainment region comprises of two distinct zones viz., transition and self-similar. In transition zone, the centerline velocity starts to decay. The velocity decay can be approximated as proportional to $x^{-0.5}$, where x is the axial distance. This usually corresponds to a region from 6d to 20d, and it is known as the interaction region where shear layers from both sides merge. In the self-similar zone, the transverse velocity profiles are similar at different values of x and the centerline velocity decay is approximately proportional to x^{-1}. Final region is the flow termination where, the centerline velocity decays rapidly to stagnation. Although this zone has been studied by several researchers, the actual mechanisms in this zone are not understood properly. It is important to note that, with distance, the efflux loses momentum and the length of core region varies under different conditions. However, the flow characteristics of jet efflux while impinging on a solid surface are very likely to alter than the free jet. The surface when placed at different locations and orientations will have significant implications. Thus, impinging jets have attracted much research from the viewpoint of the fluid flow characteristics and their influence on energy transfer. An impinging flow jet is similar to free jet and can be identified in three zones viz., free jet, stagnation, wall jet. Figure 2 shows the schematic of an impinging jet flow structure. Free jet zone represents region that is largely una□ected by the presence of the impingement surface. A potential core exists within which the jet exit velocity is conserved. A shear layer exists between the potential core and the ambient fluid which entrains ambient fluid and causes the jet to spread radially resulting lower mean velocity than the jet exit velocity. Beyond the potential core the shear layer has spread to the point where it has penetrated to the centerline of the jet. At this stage, the centerline velocity decreases drastically. Second is the stagnation zone, that extends to a radial location defined by the spread of the jet. The stagnation zone includes the stagnation point where the mean velocity is zero and within this zone the free jet is deflected into the wall jet flow. Finally, the wall jet zone which extends beyond the radial limits of the stagnation zone (figure 2).

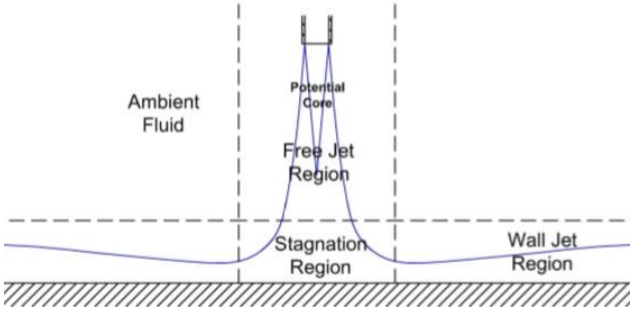

Figure 2: Schematic of an impinging flow jet regions.

Over the past six decades, jets have been the subject of extensive experimental and analytical research. In these, parameters like the jet spread rate and potential core decay play a strong role in deciding the jet effectiveness for potential applications. Therefore, understanding the fluid dynamic phenomena in the shear layer during the downstream evolution of a jet is important.

Following the classical explorations of Glauert [1] on the flow due to a jet spreading out over a plane surface, either radially or in two dimensions. The solutions of the boundary layer equations were sought and according to which the form of the velocity distribution across the jet does not vary along its length. The work explicitly obtained a similarity solution for laminar flow whereas, for turbulent flow, an eddy viscosity was introduced, and it was eventually seen that complete similarity is not attainable about the nature of the velocity distribution and the rate of growth of the wall jet. Gardon and Akfirat [2] correlated the heat transfer to an impinging jet with what is often termed the “arrival” flow condition. This is the flow condition at an equivalent location in a free jet. Jet flow characteristics are highly complex and can be influenced easily by varying flow rate, nozzle geometry, etc. Impinging jet flow characteristics are even more complicated with additional variables aecting the flow such as angle of impingement, distance from impingement surface, etc. Teles [3] worked on an axisymmetric wall jet with and without a temperature difference. A calculation procedure was devised and pronounced to predict the rate of growth, maximum velocity decay and adiabatic wall effectiveness. Comprehensive studies of the mean fluid flow characteristics of both a free and an axially symmetric impinging air jet have been presented by Donaldson and Snedeker [4], Beltaos [5] and Martin [6]. In a study by Foss [7], the mean flow properties of a jet impinging obliquely were investigated. The stagnation point for a jet impinging at an angle of 9^o was found to be displaced from the geometric center in the uphill direction. The stagnation point was further displaced from the geometric center than the location of maximum static pressure. Results for a larger angle of impingement (45^o) were presented. In this case, the location of maximum static pressure and stagnation coincide.

Several investigations varied the jet fluid to include water, oil, air and others. Obot and Trabold [8] investigated the e□ects of cross-flow as a result of confinement on the heat transfer to an array of impinging jets. The work researched nozzle geometry as a significant influence on the heat transfer. The reason was stated to be primarily due to the influence the nozzle on the turbulence level in the main jet flow. Daibes [9] worked on an incompressible, inviscid irrotational flow model to represent the normal impingement of a circular axisymmetric jet upon a flat plate. An analytical investigation was conducted to determine the free surface of the jet and the solution of the potential flow problem was obtained using finite difference techniques for jet height-to-nozzle radius ratio of 2.4. The velocity and pressure distributions at the plate surface and along the jet centerline were obtained.

The results from the finite difference solution are in close agreement with other most recent results from available experimental, and approximate solutions to the potential flow problem. The ects of nozzle geometry on the potential core length were in investigated by Ashforth-Frost and Jambunathan [10]. Four jet exit conditions were studied, namely flat and fully developed flow for unconfined and semi-confined jets. It is shown that the potential core length can be elongated by up to 7% for the fully developed flow case. This is attributed to the existence of higher shear in the flat velocity profile, leading to more entrainment of ambient fluid and therefore earlier penetration of the mixing shear layer to the center of the jet. Semi-confinement has the efect of reducing entrainment and by applying the same principle this also elongates the potential core length by up to 20%. Concurrently, Tu et. al., [11] presented comprehensive measurements of wall pressure and surface shear stress beneath a plane, two-dimensional, turbulent jet impinging normally onto a flat surface. Controlling parameters viz., Reynolds number and ratio of impingement height (H) to nozzle gap (D) (H/D) were varied in a wider range. The pressure distributions were approximated to be nearly Gaussian, independent of Reynolds number, and closely balanced the momentum flux as H/D varied. The shape of the wall shear stress distributions depended both on H/D and on Reynolds number. Results were noted to be in disagreement with the relation between wall pressure and shear stress from Hiemenz's theoretical solution for stagnation flow. It was postulated that the discrepancy is due to the relatively high free-stream turbulence level in the jet. Mehta and Prasad [12] experimented flow structure of an under-expanded and over-expanded supersonic jets impinging on an axisymmetric deflector. Particularly, effects of exit Mach number, expansion ratio, distance between nozzle exit plane to the apex of the deflector on the flow structure of the jets was studied. The work characterized discontinuities viz., jet shock, jet boundary, Mach disk, reflected shock and cone shock. The vortex formation was noted when the jet impinges on the deflector surface. The experimental static pressure distribution along the deflector wall was validated with the conforming numerical results.

Choi et. al., [13] carried out an experimental study of fluid flow and heat transfer for jet impingement cooling on a semicircular concave surface. The distributions of mean velocity and velocity fluctuation on the concave surface was measured for the cases of free, impinging and wall jet flow regions by using a Laser Doppler Anemometer. The work emphasized on measuring turbulent jet flow characteristics including impinging and evolving wall jets and interpreting heat transfer data, particularly, the occurrence and its location of secondary peak in connection with data of measured mean velocity and velocity fluctuations on the concave surface. Results stated that the potential core length becomes shorter for higher Reynolds number. The effect of fluid acceleration was observed. The occurrence of secondary peaks and their locations have been explained from the variation of measured velocity fluctuations of the wall jets evolving along the streamwise direction. Chung et. al., [14] performed Direct Numerical Simulations of an unsteady impinging jet to study momentum and heat transfer characteristics. The unsteady compressible Navier–Stokes equations was solved using a high-order finite di□erence method with non-reflecting boundary conditions. It was found that the impingement heat transfer is very unsteady and the unsteadiness is caused by the primary vortices emanating from the jet nozzle. These primary vortices were noted to dominate the impinging jet flow as they approach the wall. A detailed analysis of the instantaneous flow and temperature fields was performed showing that the location of primary vortices significantly a□ects the stagnation Nusselt number. Near the secondary vortices, the breakdown of the Reynolds analogy was observed. O'Donovan [15] concerned the measurement of heat transfer to an impinging air jet over a wide range of test parameters viz., Reynolds Numbers, nozzle to impingement surface distance H/D, and angle of impingement. Both mean and fluctuating surface heat transfer distributions from the geometric center of the jet were reported. The time averaged heat transfer distributions were qualitatively compared to velocity flow fields. Simultaneous velocity and heat flux measurements were reported at various locations on the impingement surface to investigate the temporal nature of the convective heat transfer. It was found that, at low nozzle to impingement surface spacings the heat transfer distributions exhibit peaks at a radial location that varied with both Reynolds number and H/D. The fluctuations in the velocity normal to the impingement surface were reported to have a greater influence on the heat transfer than fluctuations parallel to the impingement surface. At certain test configurations vortices that initiate in the shear layer impinge on the surface and move along the wall jet before being broken down into smaller scale turbulence. Sakakibara et. al., [16] reported, when an axisymmetric under-expanded jet impinges on a flat plate perpendicularly, the feedback mechanism of the sound waves in the flow field is known to cause the oscillation of jet

with strong noise generation. The effect of the wall jet on the oscillation mode of the impinging jet was detailed. An under-expanded wall jet was modelled as radial jet. A radial underexpanded jet issuing from a slit nozzle, consisting of two circular tubes, face to face each other, was studied experimentally and numerically. In the experimental shadowgraph picture, it was found that some ring-shaped shocks appear around the nozzle and that the local deformations of the rings occur. Sinusoidal oscillation of jet caused by many vortices was shown and local distortion of shock ring was derived by the phase difference of the oscillation in the circumferential direction. In addition, the density waves moving around the jet and forming the feedback loop were captured by computation and they transmit the information about phase difference toward upstream. As a result, such behavior of radial jet can be considered to be one of factors of the spiral motion in case of the impinging jet. Ostheimer and Yang [17] carried out numerical study on a very complicated three-dimensional (3D) flow field beneath a Vertical/Short Take-Off and Landing (VSTOL) aircraft when it is operated near the ground. The flow field was represented by the configuration of twin impinging jets along the spanwise direction in a cross-flow. The numerical results were validated against experimental data and the mean velocity profiles was reasonably well predicted. However, the Reynolds stress prediction by the Reynolds Stress Model (RSM) fair poorly compared with the experimental data, indicating that to capture the detailed unsteady flow features an LES is needed. Tiwari et. al., [18] carried out an experimental exploration to know the effects of center wall orientation effect on flow characteristics of an impinging jet. The work concluded that the increase in wall orientation axially enhances the velocity losses beyond a critical distance. The nearby exit wall orientation results in strong flow deflection resulting formation of vortices with more chances of back flow. For a fixed wall orientation, increase in radial distance enhances the velocity losses, but it results in diminishing returns beyond a critical value indicating insensitiveness of wall orientation after a certain distance. Tsun-Lirng et.al., [19] studied the impinging jet technology to provide more efficient cooling mechanism for rotating machinery. Conducted in normal condition, the experiment compared the motor's temperature change with the traditional cooling system and jet flow cooling system, at varying rotational speed of 3000rpm, 3500rpm, 4000rpm and 4500rpm. In the experiment, the motor's structure was not modified and the plates of different numbers of holes were separately added between the fan and the cooling channel. The thermocouple recorded the temperature change on the surface of the motor. The experiment concludes that the temperature on the surface does drop at the four speeds when the multi-ring and multi-hole jet plate is applied indicating that the cooling system actually works better.

On physics, the jet flow characteristics are highly complex and consequently the related energy transfer and transformation from a surface subject to such a flow is highly variable. Numerous jet configurations have been studied and numerous experimental parameters exist that influence the fluid flow and the heat transfer. The viscous forces underlying in a small flow area are of minor importance, so that potential flow theory gives results adequate for most applications. Solutions to these problems have been shown to agree closely with experimental measurements in regions where accelerations and velocities of the flow are relatively high, thus permitting practical applications of the mathematical research in this area. However, impinging jet flow problems have proved to be so formidable that researchers have been forced to obtain approximate solutions by numerical techniques or other approximate methods rather than solving the problems in closed form.

Present work explores the flow characteristics of an impinging jet against varying side wall orientation and centerwall location. This aspect of jets is yet to be comprehensively explored. Hence, a systematic study is presented to recognize mechanisms controlling the behavior of jets impinging on a wall placed at different locations and side walls at different orientations. The interest in this class of problems is specifically driven by the need to have better understanding of fluid and thermal characteristics of jets. The primary objective of the work is to conduct a fundamental investigation into air jet impingement fluid flow. To address the above-mentioned issue, the present work experimentally:

a) Explores the effects of center wall location and side walls orientation on flow characteristics of an impinging jet in a confined space.
b) Analyzes the role of key controlling parameters.

2. EXPERIMENTAL SETUP AND SOLUTION METHODOLOGY

A simple apparatus (Figure 3) was adapted and modified for present study. The apparatus consisted of a) cascade tunnel (Fig. 3(a) with base made of mild steel b) a Pitot tube (Fig. 3(a) and digital Micro Manometer (Fig. 3(b)). The cascade tunnel issues a free air jet using a centrifugal blower with a velocity of ~**36 m/s**. The efflux is from a small rectangular opening (**30 cm × 9 cm**) into the air in a quiescent room. The efflux impinges on the selected surface assembly made up of cardboard surface comprising of a central wall with dimensions of **180 cm × 120 cm × 1 cm** and joined on either side by walls of dimension **113 cm × 104 cm × 1 cm** each (figure 3(c)). When the location of central wall is varied, the entire structure moves concurrently (figure 3(d)). While analyzing the results, it is well considered that the entire assembly is open from the top. However, the emphasis is put on the variation in flow characteristics and fundamentally understanding the phenomena and implications.

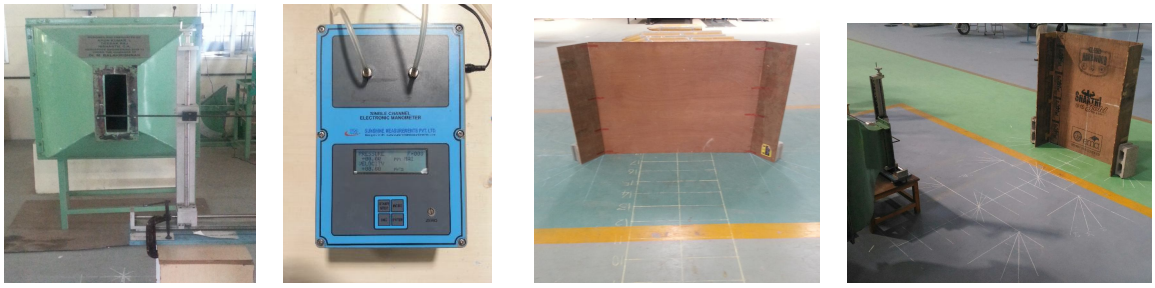

(a) (b) (c) (d)

Figure 3: Pictorial view of (a) front view of cascade tunnel (b) digital micro manometer (c) walls configuration (d) complete experimental setup.

The flow characteristics are determined by establishing the pressure balance between dynamic pressure and the hydrostatic pressure. The dynamic pressure is measured using Pitot tube (exposed directly to the flow and stagnates it at surface measuring total pressure, the static holes are at the center and side of the tube measuring static pressure and the dynamic pressure is difference of the two pressures). The micro manometer calculates the hydrostatic pressure due to change in elevation of the fluid used (here distilled water) owing to different dynamic pressures under different conditions.

The micro manometer exhibits an accuracy level of 0.001 cm height of the fluid and can measure the differential pressure up till the range of 300 mm of the used fluid. The dynamic pressure is equated to the hydrostatic pressure and the flow velocity (kinetic energy) is measured. The flow is turbulent and the effect was noted in fluctuations in the reading, so for every reading taken here the average repeated value with was accounted. The density of liquid (here distilled water) depends on the place of use of the manometer (the atmospheric pressure and temperature at the time and place of use). While, the density of air can be calculated using the state relations for air for corresponding pressure and temperature.
The flow velocity is obtained by equating the dynamic head to pressure head obtained by the liquid height change as:

$$\frac{1}{2}\rho_a V^2 = \rho_l\, g(h_1 - h_o) \qquad (1)$$

From equation (1), the flow velocity "*V*" is determined as

$$V = \sqrt{2\frac{\rho_l}{\rho_a} g\,(h_1 - h_o)} \qquad (2)$$

Where,

ρ_a Density of air (Kg/m^3)
ρ_l Density of water (Kg/m^3)
h_0 Reading corresponding to zero differential pressure
$h_1 - h_0$ Liquid head corresponding to the dynamic head
V Flow velocity (m/s)
g Gravitational acceleration (m/s^2)
D Equivalent diameter of a circular exit (**1D =18.54 cm**)

It is important to note that all the readings were taken systematically in proper time interval and all the reading taken here represent the repeatability of results obtained.

3. RESULT AND DISCUSSION

An experimental parametric study was carried out to understand the flow characteristics of flow jet issued from a small opening and impinging on a confined surface assembly with central wall placed normal at different locations and side walls at varying orientations. The coupling effect was investigated in capacity of placing the entire assembly at three different locations viz. far away from exit (12D), at an intermediate distance (10D) and at location where the assembly lies very close to exit (0D to 5D). Here, 'D' normalizes the streamline distance and all the readings were taken in folds of 'D'. It must be noted that 'D' represents the equivalent diameter of a circular exit when compared to the exit of rectangular cascade tunnel. Prior to the main study, the experimental predictions of the experimental setup were

validated with the benchmark fluid dynamics theory of a free jet. Figure 4 shows the variation of normalized centerline velocity as a function of normalized streamline distance for a free jet. The efflux at different locations is normalized by maximum velocity and the streamline distance is normalized by the equivalent circular diameter 'D'.

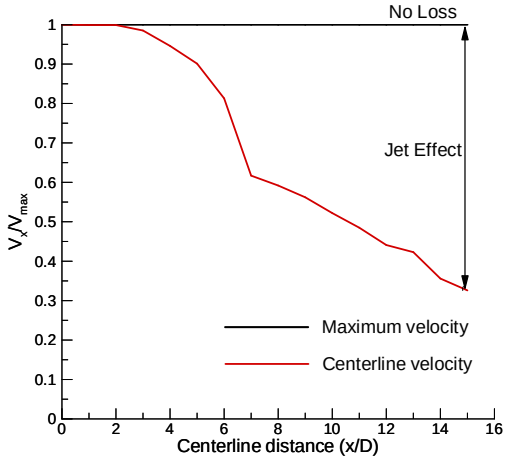

Figure 4: Variation of normalized centerline velocity as a function of normalized streamline distance for a free jet.

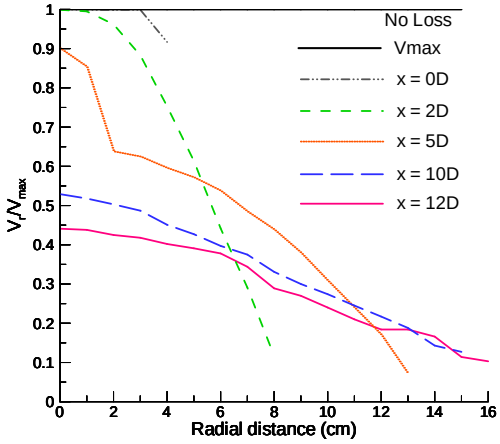

Figure 5: Variation of normalized radial velocity as a function of radial distance for a free jet.

Flow characteristic were noted to exhibits a monotonic reducing behavior with increment in streamline distance. Looking at the plot one can note that the as the jet exits the tunnel, there is drastic loss of flow velocity (kinetic energy) with increase in streamline distance. The core region was seen to extend till 2.5 units. Alongside, the axial variation of a free jet, the variation of flow velocity in radial direction at various orientations (at differential of 5 mm) is investigated. Figure 5 shows the variation of normalized velocity with distance in radial direction at selected axial locations of 0D, 2D, 5D, 10D and 12D respectively. Trend similar to axial direction was observed with the reduction in flow velocity subjected to width of core region (here noted as 3 cm). The reason for above mentioned changes in axial and radial direction can be attributed to the shear interaction with surroundings leading to strong energy conversions. The length and width of core region dictates the velocity loss at different positions. The experimental predictions match reasonably well with the preceding flow theories, the study was extended to investigate the coupling effect of centerwall location and side wall orientations on flow characteristics of an impinging flow jet.

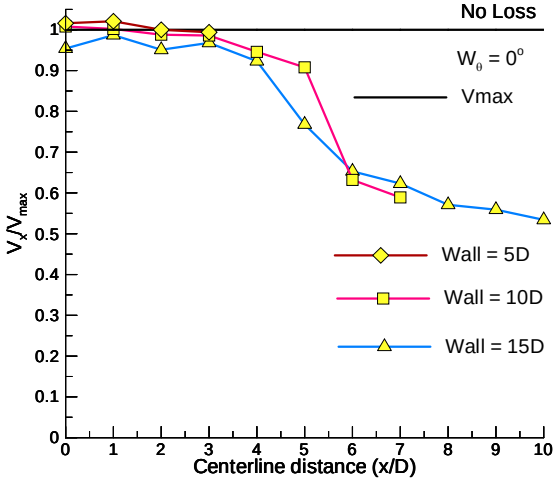

Figure 6: Variation of normalized centerline velocity as a function of normalized streamline wall location.

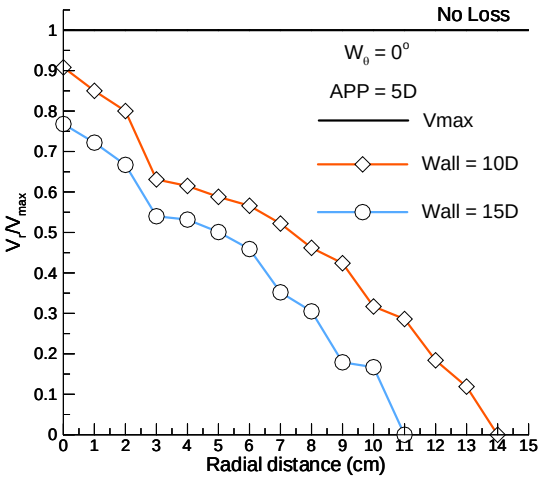

Figure 7: Variation of normalized radial velocity at as a function of radial distance at location of 5D.

First, the wall effect was investigated in the capacity of centerline against the flow at three different locations viz., very near to exit (0D & 5D), at an intermediate distance (10D), at a location far away from the exit (15D) respectively. Figure 6 shows variation of normalized centerline velocity as a function of streamline wall location in comparison to the maximum velocity (No effect). Looking at the plot one can note that, qualitatively a trend similar to free jet is

observed as the centerline velocity drops indicating the momentum loss. With the increment in the central wall location, the momentum loss was noted to increase. The velocity profiles were seen to merge and overlap for selected locations. It is interesting to note that the momentum loss at 10D wall location is lower at 6D and 7D but, in 15D the value is higher which indicates the flow resistance or presence of consequential flow. This dictates that up to a fixed wall location, the effect of shear interaction is within a closer range but as wall location increases, it behaves as a case of free jet. The core region signified by "*VRM-PPT*" point (loss in kinetic energy is less than equal to 10%) refers to the position up-till which the core region exists in streamline and radial direction as (Here 3 units= ~ 56 cm). For present case, till centerline distance of 3 units, the flow velocity loss is lower for all profiles indicating the presence of core region. A trend similar to far located wall (15D) was noted at a location of 10D. Beyond "*VRM-PPT*" point sharp drop in flow velocities is noted as all profiles fall drastically. Interestingly, at certain centerline distance, the velocity profiles converge to corroborate the loss. For wall located at 10D, the applicability of the flow can be more in comparison to the wall placed far away as the loss. The wall located close to exit paves way for strong deflection of flow and formation of vortices. The presence of walls on the sides acts as obstruction to the flow resulting in formation of vortices reducing the momentum of flow which as a consequence limits the applications of the flow jets. Owing to reduction in kinetic energy due to shear interaction with surroundings, the governing features like vortices formation and flow deflection are believed to play an important role in alteration of flow characteristics. While, when the assembly (here central wall) is placed at some intermediate viz.,10D, the reduction in flow momentum is minimized to a low level depicting stronger vortices and back flow existence which facilitates better mixing. This effect was noted to increase as the assembly was placed closed to the exit. However, with this the chances of back flow with flow coming back to exit portion are strong.

To understand the results in Figure 6, we next explore the effect of varying wall location on radial component of velocity. Figure 7 shows variation of normalized radial velocity as a function of radial distance for varying wall location. The effect in radial direction is catapulted at axial location of 5D for centerwall located at 10D and 15D respectively. The velocity profiles are similar in comparison to the centerline velocity. Looking at the profiles, one can note that "*VRM-PPT*" point exists till radial distance of 1 cm for the wall at 15D and 2 cm for 10D. A gradual drop till radial limit of "*VRM-PPT*" point is noted followed by the sharp drop.

Wall locations of 10D and 15D almost follows same trend showing insensitiveness beyond a critical value. The study substantiates the core region as 2.5 units in axial direction and 1cm in radial direction. The above-mentioned result shows that the "*VRM-PPT*" point is low in comparison to flow impinging on a single wall. The above-mentioned fact indicates that, beyond a certain location the losses are insignificant to the wall position as most of the profiles look similar and follows same trend. The reason for this can be attributed to the shear interaction of flow as it starts expanding. The presence of walls edicts vortices formation which results in increased flow losses. When central wall is placed far away the exit, the flow reaches the wall location with reduced momentum. The presence of walls on sides restricts the flow expansion and brings the flow to a stationary state which results in flow losses as efflux impinges the assembly. In the radial direction, profiles are more affected when the assembly is placed closer to the exit. Similarly, when central wall is placed far away the radial component becomes insensitive after some distance.

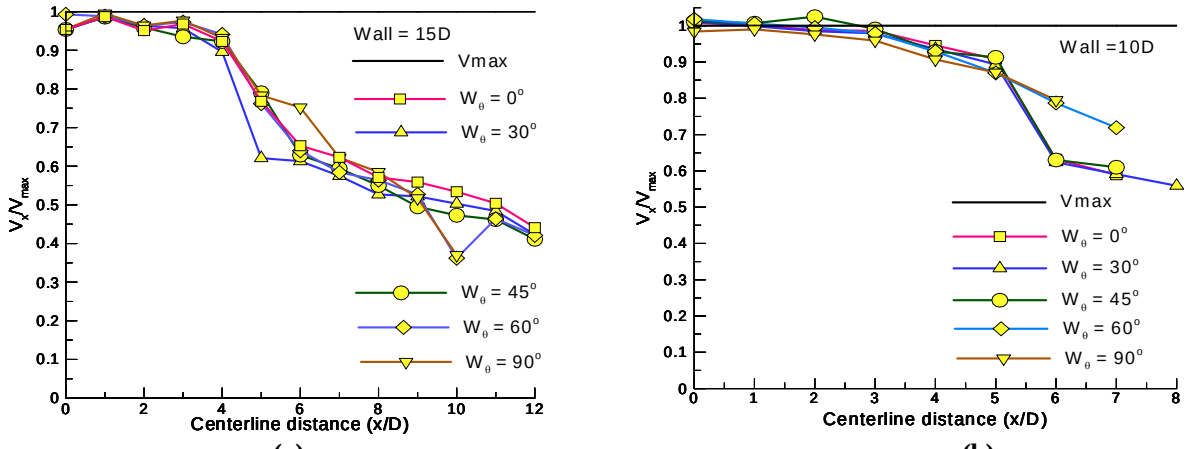

Figure 8: Variation of normalized central line velocity at wall location of (a)15D and (b) 10D as a function of side wall orientation.

Next, we look at the variation of streamline velocity with varying side wall orientation. Figure 8(a) highlights the variation for centerwall at 15D. The "*VRM_PPT*" point was noted to increase for all orientation up to 4D. However, the velocity profile took a sudden drop at axial location of 10D for 60^o and 90 ^{o} and regains the pattern with increase in distance. The reason for above changes may be attributed to the assisting area of the side walls and the distance from the exit. The resolute coupling of varying side wall orientation at a fixed center all location affects the strength of vortices which affects flow redirection. Figure 8(b) shows the variation of central line stream velocity at wall location 10D with varying orientation of the wall. It is worthwhile to note the flow behavior with side walls at 30^o stating strong energy transformation. The behavior indicates disproportionate flow resistance owing to intermittent back flow and increased entrainment region but at a lower velocity. While, at 90^o and 60^o flow disperses easily and early then other orientations. The reason attributed to this phenomenon can be the movement of the stagnation point which was created on the wall and the area of the wall which dissipates the flow. The flow hitting the wall have a less area to face and this cause a deflected flow which further disturbs the incoming flow. The molecule interaction increased with the increased in the orientation. The outer molecule transfers the heat to the inner region which is termed as the cascading of the energy and this lead to the maximum momentum to the center line. As soon as the wall orientation changes the stagnation point move from the center of the wall to the edge of the wall. This lead the heat transfer along with the deflected flow with further interacts with the incoming and hence enhancement of the momentum due to this heat transfer is seen. The next wall location was 5D where at any wall orientation the flow remains in "*VRM-PPT*" point. It also dictates that the "*VRM_PPT*" extent up to 5D (figure 9). The flow analysis was replicated in radial direction. For radial distance velocity profile follows a drop in the velocity with distance. The "*VRM-PPT*" for all orientation is found to be at 5cm. The other point to note is that the increase in orientation show less resistance from the flow and reduced radial distance.

The distance between the wall and the apparatus is very close in this case. The variation of side wall orientation does not yield significant changes in the flow momentum. Figure 9(b) shows a schematic of the resultant flow with a fixed center wall and oriented side wall. The physics of this coupling rests on the principles of flow regaining equilibrium and flow redirection owing to the side wall orientation. The flow behavior with center wall placed in the far away zone with variation in side wall orientation is unlike the centerwall location in the intermediate and nearby zone. The phenomenon is governed by the flow deflection and strength of vortices formation viz., the effect at same center wall location with side walls at horizontal and vertical orientation would never collaborate. The strength of this coupled effect owing to flow deflection and recirculation zone formation are likely to have significant implications and is termed as the "*lihze effect*" signifying the diverse flow patterns owing to centerwall location and sidewall orientations.

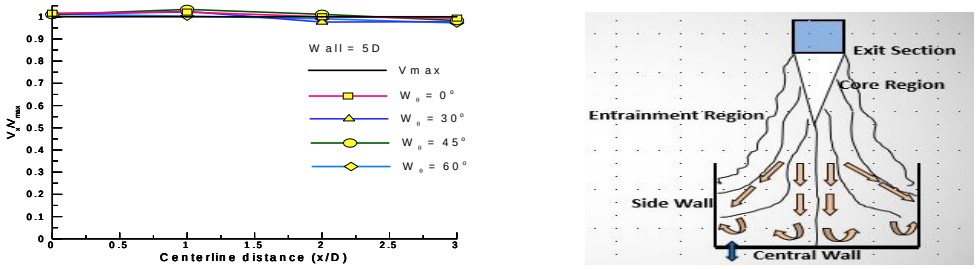

(a) **(b)**

Figure 9: Variation of normalized central line velocity at wall location of 5D as a function of wall orientation (b) schematic of the coupled centerwall and sidewall assembly.

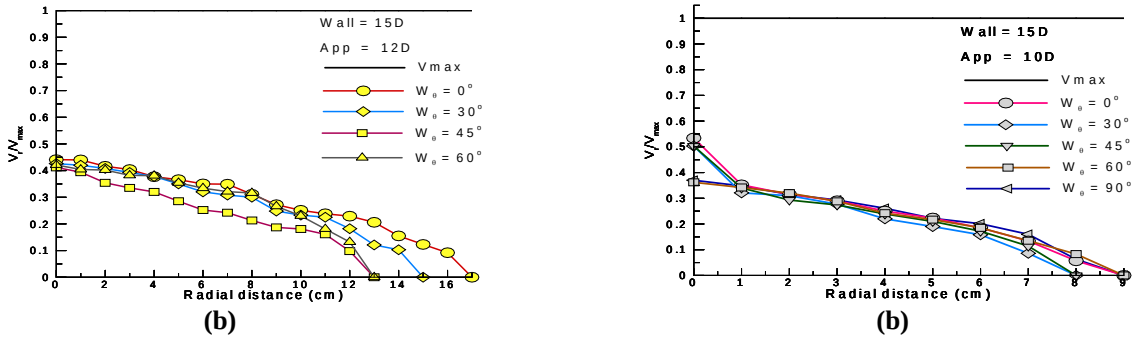

(b) **(b)**

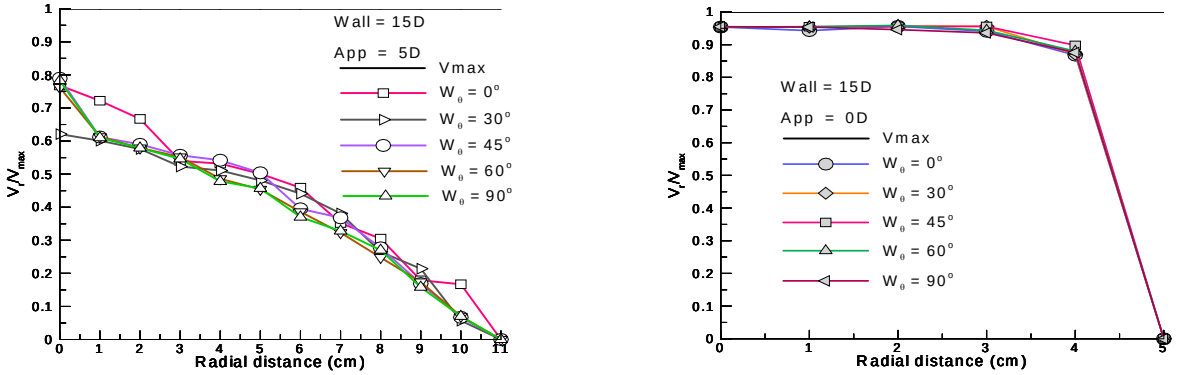

(c) **(d)**

Figure 10: Variation of normalized central line velocity at wall location of 15D and apparatus at (a)12D (b)10D (c)5D and (d)0D.

Next, we identify the effect in the radial direction to understand the shear impact upon the redirected flow. Figure 10 shows the variation of normalized radial velocity at 15D centerwall location and apparatus at (a)12D (b)10D (c)5D and (d)0D respectively. The 0^o is termed as enhancer of the flow as the resistance is high to the obstacle in the flow. Whereas the increase in the orientation increase the depletion in the flow and hence the entrainment region falls early. The placement of the wall is far from the exit nozzle i.e. (278.1 cm) whereas the apparatus to measure the flow is far too from the exit nozzle but near to the wall placement.

This arrangement shows the highest entrainment region for the 0^o in radial direction and the reason attributed to it is that the wall is flat and the apparatus can easily detect the back-flow due to the object in the flow path. The stagnation point generates on the wall which creates the sound which itself is a pressure wave. This pressure wave further leads to the increment in the temperature in the flow. The average velocity of the flow particle increases as the result increase in the entrainment region. The least value of the velocity at the central line distance i.e. 0 cm radial distance is obtained by 30^o, 60^o and 90^o. The least radial distance is obtained for 30^o and 45^o. Interestingly the value of velocity is obtained **28%** less for 30^o, 60^o and 90^o. "*VRM-PPT*" point exist for this profile only up to 1 cm radial distance for others it directly comes out of the core region. It shows the impact of the deflected flow as the velocity of the deflected flow is unidirectional and hence the incoming flow lose the momentum which further affects the velocity profile. This is the interesting part of the results which indicates 0^o and 30^o as the velocity enhancer when the wall placement is far but the apparatus is in intermediate region. The molecule interaction happens as the flow gets deflected. This deflected flow in which the molecules are well stabilized after the increment of the average velocity avails the addition momentum to the incoming flow. For the apparatus kept at 5D three different "*VRM-PPT*" point was observed with different surface orientation. For 30^o, the "*VRM-PPT*" point is up to 3cm for 0^o it is till 1cm and for rest of other it comes out of "*VRM-PPT*" point with a unit change in radial distance. For 0^o, 9 cm and 10 cm shows no effect to the distance as flow is strongly affected. As mentioned before, the increment in the distance of the apparatus and wall placement neglects the account of the increased deflected velocity. The figure shows the same entrainment region of all the orientation of the wall which indicates that the average increased flow velocity is not more than the exit velocity and hence depleted easily with the distance. For the apparatus kept at just the exit the "*VRM-PPT*" point extends up to 4 cm for all orientation. Then it drops sudden and dissipate in with environment.

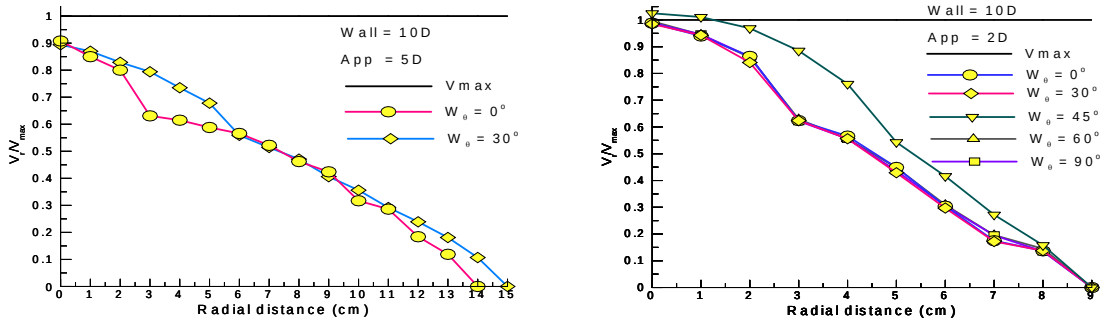

(a) **(b)**

Figure 11: Variation of normalized radial velocity with wall orientation at 10D at radial location of (a) 5D and (b) 2D.

Figure 11 details normalized radial velocity variation for centerwall located at 10D and apparatus at 5D orientation.

The "*VRM-PPT*" point was found to be 1 cm for both the orientation however, there is a sudden drop in the velocity after 2 cm for 0^o. Sidewall orientation 0^o also shows less entrainment region whereas 30^o follows a conventional pattern. The contribution of the deflected flow can be seen in 30^o wall orientation. With the wall placement at 15D and the apparatus at 5D, the entrainment region was found to be 11cm but as the wall moves to the 10D with the same location of the apparatus i.e. 5D the entrainment region increased to 15cm. The reason for above mentioned change may be attributed to the fact that the momentum loss of the flow particle is less and particle interaction due to the flow deflection interacting with the already momentum carrying flow and hence the energy transfer. Whereas, at 0^o the wall area leads and the flow dissipates in all the direction because of the stagnation point generated in the centerwall. This also shows how to use the deflected velocity in terms of application and how the energy transfers with the movement of the stagnation and pressure point which was generated on the wall due to the striking of the flow. Sidewall orientation of 45^o shows the highest value of velocity profile with the apparatus kept at 2D with value of "*VRM-PPT*" point to be 2 cm. All the side wall orientation was noted to stagnate at same radial distance i.e. 9 cm. The 45^o velocity profile can be termed as the enhancer of the flow whereas, remaining profile decreases the velocity and hence termed as resistance to the flow. The apparatus is very close to the exit and do not shows much variation in term of the entrainment length. The only variation is seen is in the term of the decrement in the flow velocity. The 45^o contributes to the incoming flow but the magnitude is very less from the exit velocity it only resists the flow from falling drastically which further enhance the "*VRM-PPT*" point. The momentum which was increased due to the shear interaction of the molecules contributes to the flow but itself depleted due to the distance of the wall placement. Figure 12 details variation of radial velocity for centerwall location of 5D. Owing to closeness to the exit, the diversity in the flow phenomenon is not in folds.

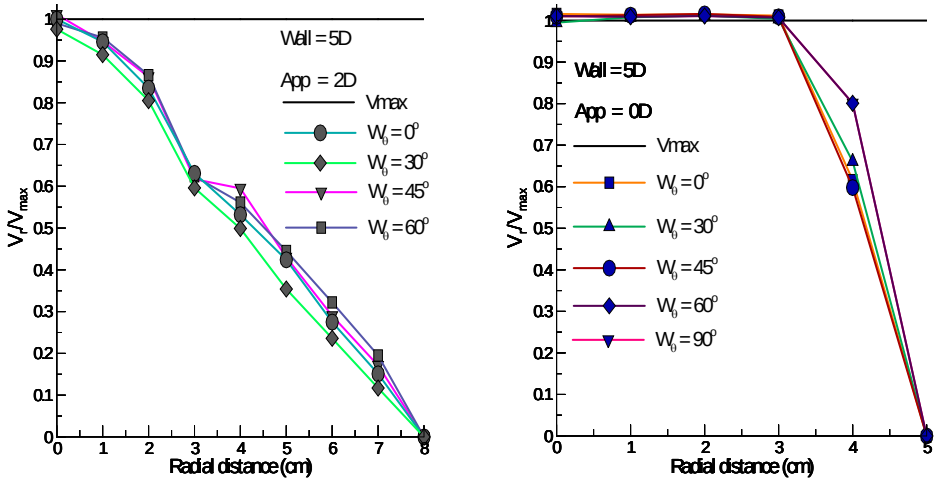

(a) **(b)**

Figure 12: Normalized radial velocity variation at (a)2D and (b) 0D for varying wall orientation at 5D.

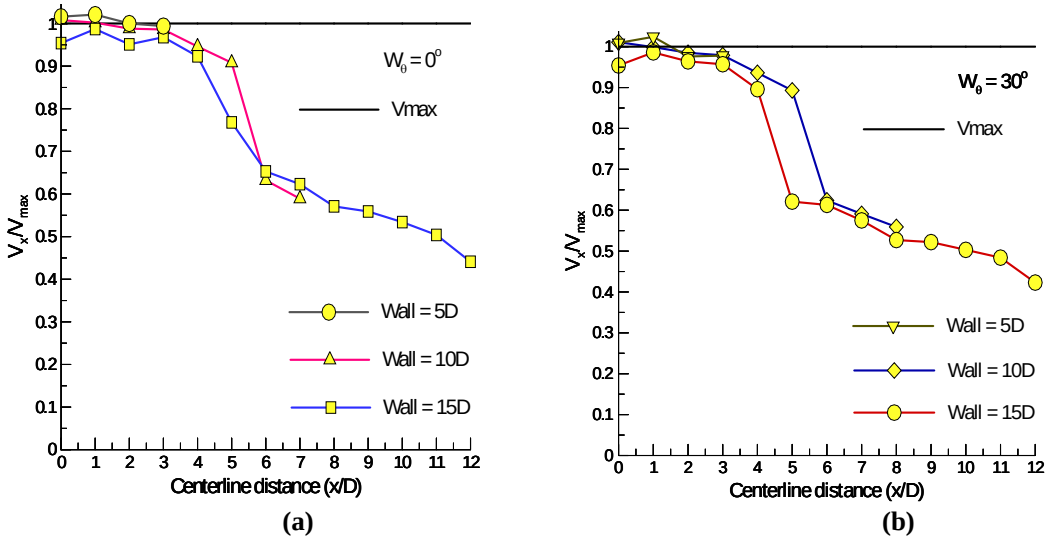

(a) **(b)**

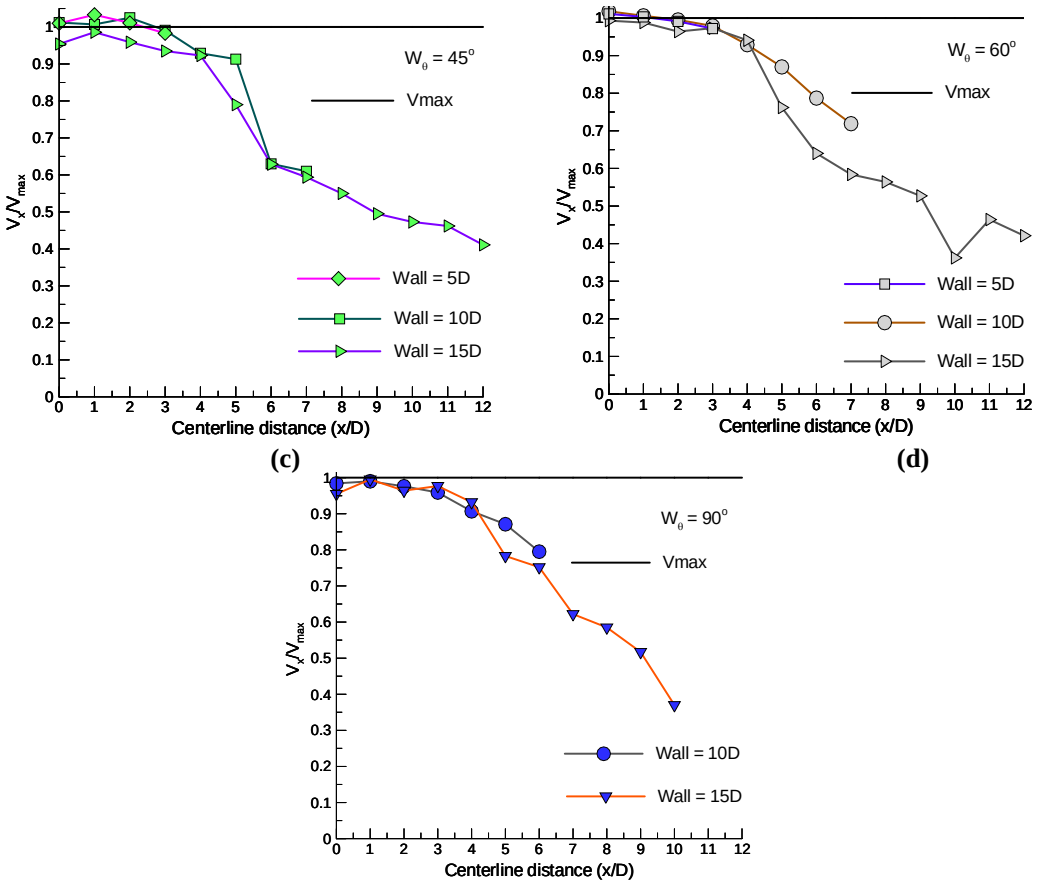

Figure 13: Variation of normalized streamline velocity with distance for varying central wall location and orientation (a) 0^o (b) 30^o (c) 45^o (d) 60^o (e) 90^o.

Figure 13 shows the centerline velocity variation for the centerwall located at selected 5D, 10D and 15D with varying side wall orientations. The value of "*VRM-PPT*" point increases as soon we move the apparatus near the exit and the value obtained is ~4cm in radial direction. The highest core was noted for the 10D and 15D i.e. 4cm after that the velocity drops. The value of "*VRM-PPT*" point can be noted to vary with the coupling "*lihze effect*". For the wall at 5D the value is obtained till 3D and it remains in core region. The 90^o side wall orientations depicts significant momentum loss. Whereas, remaining configurations resorts to the similar flow jet behavior at selected wall orientation. The centerwall orientation of 10D show maximum resistance to the incoming flow. The value of VRM-PPT point obtained for 10D is 4cm whereas for 15D it is 3cm. The 45^o shows the maximum velocity and interestingly the enhancement of the core region is seen at the wall location of 10D. The reason attributed to this is the interaction of the deflected velocity and the incoming flow. An interesting case is with side wall orientation of 60^o depicting sudden drop at axial location of 10D. The flow which is coming itself carries a high momentum and the deflected velocity interaction creates the vortex in that region. This vortex formation dissipates the energy or the momentum of the flow which results as the less entrainment region. The increased in the distance between the wall placement and apparatus gives the space to the back flow which carries the heat and contributed it to the incoming flow. Whereas, the other orientation profiles resort to insensitiveness due to proportional shear interaction.

4. CONCLUSION

An experimental exploration was carried out to understand the coupling effect of varying wall location and side wall orientation on flow characteristics of an impinging jet. The results predicted by existing experimental setup were validated with benchmark preceding free jet theory. Based on results obtained following conclusions may be drawn from the study: The increase in centerwall location along with varying sidewall orientations results in mixed effect on flow transformation unlike wall jet and free jet. The wall location near to exit results in low velocity losses and consequently strong deflection of flow resulting formation of vortices with strong back flow. For a fixed wall location, increase in radial distance enhances the velocity losses, but it results in diminishing returns beyond a critical value indicating insensitiveness of wall orientation after a certain distance. The confined configurations result in both flow momentum enhancement and reduction beyond a critical distance (i.e., core region). The maximum diversity is

obtained at intermediate centerwall location (here 10D) and intermediate side wall orientation (45^o). The effect of coupling represents non-linearity and is termed as "*lihze effect*". The configurations can be effectively used in the wide range of industrial, practical, functional, research, scientific and engineering applications.

References

[1] Glauert, M. B., "The wall jet," Journal of Fluid Mechanics, vol. 1, pp. 625–643, 1956.
[2] Gardon, R. J., and Akfirat, J. C., International Journal of Heat and Mass Transfer, 8, pp. 1261-1272, 1965.
[3] Teles, J. C. M. G., "The turbulent axisymmetric wall jet," M.Sc. Thesis, Imperial College of Science and Technology Mechanical Engineering Department, London, 1968.
[4] Donaldson, C. D., and Snedeker, R. S., "A study of free jet impingement, mean properties of free impinging jets," Journal of Fluid Mechanics, 45, pp. 281-319, 1971.
[5] Beltaos, S., "Oblique impingement of circular turbulent jets," Journal of Hydraulic Research, 14, pp. 17-36, 1976.
[6] Martin, H., "Heat and mass transfer between impinging gas jets and solid surfaces," Advances in Heat Transfer, 13, pp. 1-60, 1977.
[7] Foss, J. F., "Measurement in a large-angle oblique jet impingement flow," AIAA Journal, 17, pp. 801-802, 1979.
[8] Obot, N. T., and Trabold, T. A., "Impingement heat transfer within arrays of circular jets: Part 1-e□ects of medium, intermediate, and complete crossflow for small and large spacings," ASME Journal of Heat Transfer, 109, pp. 872 – 879, 1987.
[9] Daibes, A. J., "Impingement of an axisymmetric jet on a flat surface" M.Sc. Thesis, New Jersey Institute of Technology, New Jersey, 1980.
[10] Ashforth-Frost, S., and Jambunathan, K., International Communications in Heat and Mass Transfer, 23, 155–162, 1996.
[11] Tu, C.V., and Wood, D. H., "Wall Pressure and Shear Stress Measurements Beneath an Impinging Jet," Experimental Thermal and Fluid Science, 13:364-373, 1996.
[12] Mehta, R. C., and Prasad, J. K., "Flow structure of a supersonic jet impinging on an axisymmetric deflector," Indian Journal of Engineering and Material Sciences, Vol. 4, pp. 178-188, 1997.
[13] Choi, M., Yoo, H. S., Yang, G., Lee, J. S., Sohn, D. K., "Measurements of impinging jet flow and heat transfer on a semi-circular concave surface," International Journal of Heat and Mass Transfer, 43, pp. 1811-1822, 2000.
[14] Chung, Y.M., Luo, K.H., and Sandham, N.D., "Numerical study of momentum and heat transfer in unsteady impinging jets," International Journal of Heat and fluid flow, 23, pp. 592-600, 2002.
[15] O'Donovan, T. S., "Fluid Flow and Heat Transfer of an Impinging Air Jet", PhD Thesis, University of Dublin, Department of Mechanical & Manufacturing Engineering, Trinity College, Dublin, March, 2005.
[16] Sakakibar, Y., Endo, M. and Iwamoto, J., "Effect of Wall Jet on Oscillation Mode of Impinging Jet", 10th FLUCOME, Moscow, Russia, 2009.
[17] Ostheimer, D., and Yang, Z., "A CFD Study of Twin Impinging Jets in a Cross-Flow", The Open Numerical Methods Journal, 4, 24-34, 2012.
[18] Tiwari, P., Mahathi, P., Choudhury, N.R., and Malhotra, V., Proc. Int. conference on recent trends in engineering and technology, Cochin, Kerala, January 18-19, 2014.
[19] Tsun-Lirng, Y., Hsien-Te, Pan, Shing-Chi, Yu., "The Experimental Study of Impinging Jet Flow Cooling Technology for Electric Motor", International Journal of Mechanical and Production Engineering, Volume- 4, Issue-2, February, 2016.